

Hadronic Uncertainties versus New Physics for the W boson Mass and Muon $g - 2$ Anomalies

Peter Athron^{1*}, Andrew Fowlie^{1†}, Chih-Ting Lu^{1‡}, Lei Wu^{1§}, Yongcheng Wu^{1¶}, Bin Zhu^{2**}

¹Department of Physics and Institute of Theoretical Physics, Nanjing Normal University, Nanjing, 210023, China

²Department of Physics, Yantai University, Yantai 264005, China

*peter.athron@njnu.edu.cn †andrew.j.fowlie@njnu.edu.cn ‡06285@njnu.edu.cn

§leiwu@njnu.edu.cn ¶ycwu@njnu.edu.cn **zhubin@mail.nankai.edu.cn

There are now two single measurements of precision observables that have major anomalies in the Standard Model: the recent CDF measurement of the W mass shows a 7σ deviation and the Muon $g - 2$ experiment at FNAL confirmed a long-standing anomaly, implying a 4.2σ deviation. Doubts regarding new physics interpretations of these anomalies could stem from uncertainties in the common hadronic contributions. We demonstrate that these two anomalies pull the hadronic contributions in opposite directions by performing electroweak fits in which the hadronic contribution was allowed to float. The fits show that including the $g - 2$ measurement worsens the tension with the CDF measurement and conversely that adjustments that alleviate the CDF tension worsen the $g - 2$ tension beyond 5σ . This means that if we adopt the CDF W mass measurement, the case for new physics in either the W mass or muon $g - 2$ is inescapable regardless of the size of the SM hadronic contributions. Lastly, we demonstrate that a mixed scalar leptoquark extension of the Standard Model could explain both anomalies simultaneously.

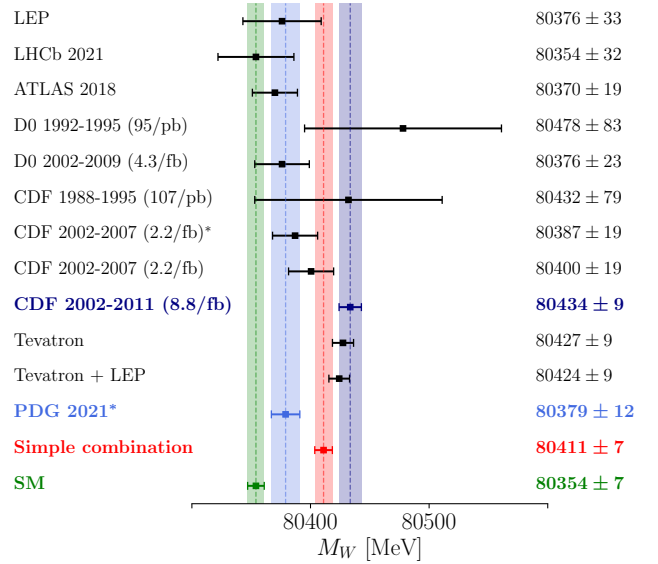
INTRODUCTION

The CDF collaboration at Fermilab recently reported the world's most precise direct measurement of the W boson mass, $M_W^{\text{CDF}} = 80.4335 \pm 0.0094$ GeV [1], based on 8.8/fb of data collected between 2002-2011. This deviates from the Standard Model (SM) prediction by about 7σ . The recent FNAL E989 measurement of the muon's anomalous magnetic moment furthermore implies a new world average of $a_\mu = 16\,592\,061(41) \times 10^{-11}$ [2], which is in 4.2σ tension with the SM theory prediction from the Muon $g - 2$ Theory Initiative, $116\,591\,810(43) \times 10^{-11}$ [3]. This prediction is based on results from Refs. [4–29].

Whilst the Fermilab $g - 2$ measurement was in agreement with the previous BNL E821 measurement [30], as shown in fig. 1 there appears to be tension between the new CDF measurement and previous measurements, including the previous CDF measurement with only 2.2/fb of data [31]. Updates to systematic uncertainties shift the previous measurement by 13.5 MeV, however, such that the CDF measurements are self-consistent. In the Supplementary Note 1 we find a reduced chi-squared from a combination of $N = 7$ measurements of about $\chi^2/(N - 1) \simeq 3$ and a tension of about 2.5σ . Nevertheless, we show that these two measurements could point towards physics beyond the SM with a common origin and, under reasonable assumptions, that the new CDF W mass measurement pulls common hadronic contributions in a direction that significantly strengthens the case for new physics in muon $g - 2$.

We now turn to the SM predictions for the W mass and muon $g - 2$. Muon decay can be used to predict M_W in the SM from the more precisely measured inputs, G_μ , M_Z and α (see e.g. Ref. [40])

$$M_W^2 = M_Z^2 \left\{ \frac{1}{2} + \sqrt{\frac{1}{4} - \frac{\pi\alpha}{\sqrt{2}G_\mu M_Z^2} (1 + \Delta r)} \right\}. \quad (1)$$



* Does not include 13.5 MeV shift in CDF 2002-2007 (2.2/fb)

Figure 1. **Simple combination of M_W measured by different experiments.** Measurements of the W boson mass from LEP [32], LHCb [33], ATLAS [34], D0 [35] and CDF I and II [1, 31, 36]. We show an SM prediction [37], the previous PDG combination of measurements [38], CDF combinations of Tevatron and LEP measurements [1], and a simple combination that includes the new measurement, which is explained in the Supplementary Note 1. The PDG combination includes uncorrected CDF measurements. The error bars show 1σ errors. The code to reproduce this figure is available at [39].

The loop corrections are contained in Δr : full one-loop contributions were first calculated in Refs. [41, 42], and the complete two-loop contributions are now available [43–60]. These have been augmented with leading three-loop and leading four-loop corrections [61–70]. The state-of-the-art on-shell (OS) calculation of M_W in the SM [40] updated with recent

data gives 80.356 GeV [71], whereas the $\overline{\text{MS}}$ scheme [72] result is about 6 MeV smaller when evaluated with the same input data. Direct estimates of the missing higher order corrections were a little smaller (4 MeV for OS and 3 MeV for $\overline{\text{MS}}$).

The predictions also suffer from parametric uncertainties, with the largest uncertainties coming from m_t and may be around 9 MeV [72], and depend on estimates of the hadronic contributions to the running of the fine structure constant, $\Delta\alpha_{\text{had}} \equiv \Delta\alpha_{\text{had}}^{(5)}(M_Z^2)$, defined at the scale M_Z for five quark flavors. This is constrained by electroweak (EW) data and by measurements of the $e^+e^- \rightarrow \text{hadrons}$ cross section (σ_{had}) through the principal value of the integral [73]

$$\Delta\alpha_{\text{had}} = \frac{M_Z^2}{4\pi^2\alpha} \int_{m_{\pi^0}^2}^{\infty} \frac{ds}{M_Z^2 - s} \sigma_{\text{had}}(\sqrt{s}), \quad (2)$$

where m_{π^0} is the neutral pion mass. The parametric uncertainties may be estimated through global EW fits. For example, two recent global fits without any direct measurements of the W boson mass predict 80.354 ± 0.007 GeV [37] and 80.3591 ± 0.0052 GeV [74] in the OS scheme. Lastly, the CDF collaboration quote 80.357 ± 0.006 GeV [1]. While the precise central values and uncertainty estimates vary a little, all of these predictions differ from the new CDF measurement by about 7σ .

Turning to muon $g - 2$, the SM prediction for a_μ includes hadronic vacuum polarization (HVP) and hadronic light-by-light (HLbL) contributions in addition to the QED and EW contributions that can be calculated perturbatively from first principles [3]. Although HVP is not the main contribution for a_μ , it suffers from the largest uncertainty and it is hard to pin down its size. The HLbL contributions in contrast have a significantly smaller uncertainty, with data-driven methods now providing the most precise estimates but with lattice QCD results that are consistent with these and which also contribute to the final result in Ref. [3]. Two approaches are commonly used to extract the contributions from HVP. First, a traditional data-driven method in which the HVP contributions are determined from measurements of σ_{had} using the relationship [75]

$$a_\mu^{\text{HVP}} = \frac{m_\mu^2}{12\pi^3} \int_{m_{\pi^0}^2}^{\infty} \frac{ds}{s} K(s) \sigma_{\text{had}}(\sqrt{s}), \quad (3)$$

where m_μ and m_{π^0} are the muon and neutral pion masses, respectively, and $K(s)$ is the kernel function as shown in Refs. [75, 76]. This approach results in $a_\mu^{\text{HVP}} = 693.1(4.0) \times 10^{-10}$ with an uncertainty of less than 0.6% [8–10, 12, 13, 77]. The second approach uses lattice QCD calculations. The recent leading-order lattice QCD calculations for HVP from the BMW collaboration significantly reduced the uncertainties and resulted in $a_\mu^{\text{HVP}} = 707.7(5.5) \times 10^{-10}$ [78]. This, however, shows tension with the σ_{had} measurements method.

The M_W and muon $g - 2$ calculations are in fact connected by the fact that both $\Delta\alpha_{\text{had}}$ and the HVP contributions can be extracted from the hadronic cross section, $\sigma_{\text{had}}(\sqrt{s})$, through

eqs. (2) and (3). We assume that the energy dependence of this cross-section, $g(\sqrt{s})$, is reliably known for $\sqrt{s} \geq m_{\pi^0}$ [9, 12], but that the overall scale, σ_{had} , may be adjusted,

$$\sigma_{\text{had}}(\sqrt{s}) = \sigma_{\text{had}} g(\sqrt{s}). \quad (4)$$

This simple modification is similar to scenario (3) in Ref. [73]. There are of course more complicated possibilities, including increases and decreases in the hadronic cross section at different energies. Ref. [79] considered these complicated possibilities to be implausible, though this is a somewhat subjective matter; see Supplementary Note 2 for further discussion. Using eqs. (2) and (4) we may trade σ_{had} for $\Delta\alpha_{\text{had}}$ giving $\Delta\alpha_{\text{had}} \propto \sigma_{\text{had}}$. The HVP contributions depend on $\Delta\alpha_{\text{had}}$ and conversely estimates of the HVP contributions from either hadronic cross-sections or lattice QCD constrain $\Delta\alpha_{\text{had}}$. Further details of the transformation between $\Delta\alpha_{\text{had}}$ and a_μ^{HVP} are provided in the Supplementary Note 2. Thus we can transfer constraints on $\Delta\alpha_{\text{had}}$ from measurements of M_W to constraints on the HVP contributions to muon $g - 2$ and vice-versa [79–81] through global EW fits.

In this work, we study how the new M_W measurement from CDF impacts estimates of muon $g - 2$ in global EW fits and show that a common explanation of muon $g - 2$ and the CDF M_W from hadronic uncertainties are not possible. Then we demonstrate that in contrast a scalar leptoquark model could provide a simultaneous explanation of both muon $g - 2$ and the W mass anomalies.

RESULTS AND DISCUSSION

Electroweak Fits of the W mass and Muon $g - 2$

We first investigated the impact of the W mass on the allowed values of $\Delta\alpha_{\text{had}}$ by performing EW fits using `Gfitter` [37, 82–85] with data shown in Supplementary Table 1 where m_h , m_t , M_Z , α_s and $\Delta\alpha_{\text{had}}$ were allowed to float. The Fermi constant $G_F = 1.1663787 \times 10^{-5}$ GeV $^{-2}$ and the fine-structure constant $\alpha = 1/137.035999074$ [86] in the Thompson limit were fixed in our calculation. Although $\Delta\alpha_{\text{had}}$ is not a free parameter of the SM as it is in principle calculable, it isn't precisely known and so we allowed it to float, following the approach used in Ref. [73]. We found the allowed $\Delta\alpha_{\text{had}}$ when assuming specific W masses between 80.3 GeV and 80.5 GeV; the results form the diagonal red band in fig. 2. We fixed $\Delta M_W = 9.4$ MeV when obtaining the $\pm 1\sigma$ region. The previous world average (PDG 2021) and current CDF measurement (CDF 2022) of the W mass are shown by blue and green vertical bands, respectively, and the corresponding best-fit $\Delta\alpha_{\text{had}}$ are indicated by blue and green dashed horizontal lines, respectively. From the intersection of regions allowed by CDF 2022 (green) and the EW fit (red), we see that the CDF measurement pulls $\Delta\alpha_{\text{had}}$ down to about 260×10^{-4} , making the muon $g - 2$ discrepancy even worse. Indeed, unless the CDF measurement is entirely disregarded it must in-

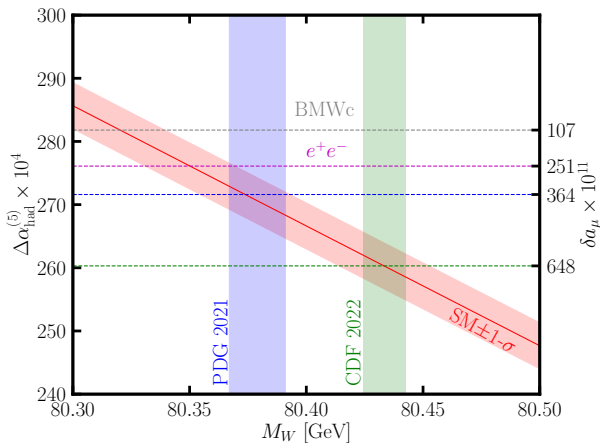


Figure 2. **Correlation of $\Delta\alpha_{\text{had}}$ with M_W in the electroweak fits.** The allowed values of $\Delta\alpha_{\text{had}}$ assuming specific values of the W boson mass in the SM found from EW fits. The solid line indicates the central value from the fit without any input for $\Delta\alpha_{\text{had}}$, while the red band shows the 1σ region. The current world average (PDG 2021) and new measurement (CDF 2022) for M_W are indicated by vertical bands. We indicate the favored $\Delta\alpha_{\text{had}}$ from BMW lattice calculations (gray), e^+e^- cross section measurements (magenta), our fit using M_W from PDG 2021 (blue) and our fit using M_W from CDF 2022 (green).

crease the tension between the muon $g-2$ measurements and the SM prediction. The overall best-fits were found at around $M_W \approx 80.35$ GeV, in agreement with previously published fits.

We further scrutinize the impact of assumptions about the HVP contributions and the W mass through several fits shown in table I. In the first three fits, the W mass is only indirectly constrained by EW data, and $\Delta\alpha_{\text{had}}$ is constrained by the BMWc determination of the HVP contributions, by the e^+e^- data, and indirectly by EW data. The second and final three fits are similar, though the W mass is constrained by the PDG 2021 world average and by the CDF 2022 measurement, respectively. In each case we show the overall goodness of fit, and how much the best-fit muon $g-2$ and W mass predictions deviate from the world average and the recent CDF measurement, respectively. Regardless of the constraints imposed on $\Delta\alpha_{\text{had}}$, including the CDF measurement results in poor overall goodness of fit and increases the tension between the SM prediction for $g-2$ and the world average. The tension between the SM prediction for the W mass and the CDF measurement range from 3.2σ to 7.8σ . However, the former occurs only when estimates of HVP are completely ignored (final column) and at the expense of increased tension in the SM $g-2$ prediction and a poor overall goodness of fit. Note that this includes the scenario where we do not include any input values for M_W or $\Delta\alpha_{\text{had}}$ in the global EW fit, as shown in the third data column (of twelve). Even in this case there is still a large tension with the CDF measurement (5.8σ), indicating that other EW observables also constrain $\Delta\alpha_{\text{had}}$. Using the e^+e^- estimates of HVP, which is a standard choice, we see about 5σ tension in both $g-2$ and the W mass. In fact, the

CDF measurement takes the tension between the SM prediction for muon $g-2$ and the measurements slightly beyond 5σ . Switching to BMWc estimates of HVP partially alleviates the tension in $g-2$ but results in increased tension with the CDF W mass measurement.

In summary, our fits showed the extent to which the new W mass measurement worsens tension with muon $g-2$, using the reasonable assumption that the energy-dependence of the hadronic cross section that connects these is well-known and not modified by for example very light new physics. The anomalies pull $\Delta\alpha_{\text{had}}$ in opposite directions in EW fits, making it even harder to explain both within the SM. We thus now turn to a new physics explanation.

Interpretation in Scalar Leptoquark Model

Even without light new physics, sizable BSM contributions to muon $g-2$ can be obtained by an operator that gives an internal chirality flip in the one-loop muon $g-2$ corrections (see e.g. Refs. [87, 88] for a review). On the other hand, BSM contributions to the W mass can be obtained when there are large corrections to the oblique parameter T [89]. We show that a scalar leptoquark model can satisfy both of these criteria and provide a simultaneous explanation of both muon $g-2$ and the W mass anomalies. We anticipate other possibilities, including composite models with non-standard Higgs bosons [90].

Scalar leptoquarks (LQs) (see Ref. [91] for a review), or more specifically the scalar leptoquarks referred to as S_1 ($\bar{3}, 1, 1/3$) and R_2 ($3, 2, 7/6$) in Ref. [92–94], are well known to provide the chirality flip needed to give a large contribution to a_μ [95], and have also been proposed for a simultaneous explanation of the flavour anomalies [96]. Furthermore due to the mass splitting between its physical states the SU(2) doublet R_2 is capable of making a considerable contribution to the W mass. However we find that the mass splitting from a conventional Higgs portal interaction cannot generate corrections big enough to reach the CDF measurement, unless the interaction $\lambda_{R_2 H R_2^\dagger} H H^\dagger R_2$ is non-perturbative. We thus analyze the plausibility of situations in which one-loop contributions to the anomalous muon magnetic moment and W mass corrections are created via the mixing of two scalar LQs through the Higgs portal. For simplicity, we consider the S_1 & S_3 ($\bar{3}, 3, 1/3$) scenario,

$$\mathcal{L}_{S_1 \& S_3} = \mathcal{L}_{\text{mix}} + \mathcal{L}_{\text{LQ}}, \quad (5)$$

where the first term is responsible for the mixing of the two LQs, and the second specifies the interaction between quarks and leptons

$$\mathcal{L}_{\text{mix}} = \lambda H^\dagger \left(\vec{\tau} \cdot \vec{S}_3 \right) H S_1^* + \text{h.c.} \quad (6)$$

$$\mathcal{L}_{\text{LQ}} = y_R^{ij} \bar{u}_{Ri}^C e_{Rj} S_1 + y_L^{ij} \bar{Q}_i^C i\tau_2 \left(\vec{\tau} \cdot \vec{S}_3 \right) L_j + \text{h.c.} \quad (7)$$

M_W		Indirect			PDG 2021			CDF 2022			Simple Combination		
$\Delta\alpha_{\text{had}}$		BMWc	e^+e^-	Indirect	BMWc	e^+e^-	Indirect	BMWc	e^+e^-	Indirect	BMWc	e^+e^-	Indirect
Input	M_W [GeV]	-	-	-	80.379(12)	80.379(12)	80.379(12)	80.4335(94)	80.4335(94)	80.4335(94)	80.411(7)	80.411(7)	80.411(7)
	$\Delta\alpha_{\text{had}} \times 10^4$	281.8(1.5)	276.1(1.1)	-	281.8(1.5)	276.1(1.1)	-	281.8(1.5)	276.1(1.1)	-	281.8(1.5)	276.1(1.1)	-
χ^2/dof		18.32/15	16.01/15	15.89/14	23.41/16	18.74/16	17.59/15	74.51/16	62.58/16	47.19/15	62.08/16	49.79/16	35.48/15
Fitted	M_W [GeV]	80.348(6)	80.357(6)	80.359(9)	80.355(6)	80.361(6)	80.367(7)	80.375(5)	80.380(5)	80.396(7)	80.377(5)	80.381(5)	80.393(6)
	$\Delta\alpha_{\text{had}} \times 10^4$	280.9(1.4)	275.9(1.1)	274.4(4.4)	280.3(1.4)	275.6(1.1)	271.7(3.8)	278.6(1.4)	274.7(1.0)	260.9(3.6)	278.5(1.4)	274.6(1.0)	262.3(3.4)
	$\delta a_\mu \times 10^{11}$	-	-	294(166)	146(68)	264(59)	364(145)	188(68)	289(57)	648(137)	191(68)	289(57)	597(132)
	Tension	-	-	1.8 σ	2.1 σ	4.5 σ	2.5 σ	2.8 σ	5.1 σ	4.7 σ	2.8 σ	5.1 σ	4.5 σ
	δM_W [MeV]	86(11)	77(11)	75(13)	79(11)	73(11)	67(12)	59(11)	54(11)	38(12)	57(11)	53(11)	41(11)
	Tension	7.8 σ	7.0 σ	5.8 σ	7.2 σ	6.6 σ	5.6 σ	5.4 σ	4.9 σ	3.2 σ	5.2 σ	4.8 σ	3.7 σ

Table I. SM predictions from EW fits for $\Delta\alpha_{\text{had}}$ and M_W , and the differences with respect to measurements of muon $g-2$ and the W mass, δa_μ and $\delta M_W \equiv M_W^{\text{CDF}} - M_W$. The input data for $\Delta\alpha_{\text{had}}$ and M_W are listed in first two rows for each case.

Although a coupling between S_1 and the left-handed lepton and quark fields is also allowed, we do not initially consider it here. Instead we show that it is possible to have new physics explanations of the CDF 2022 measurement and the 2021 combined a_μ world average that originate from the same feature of the model, namely the combination of the S_1 and S_3 states through a non-vanishing mixing parameter, λ . For simplicity, we assume that only the couplings to muons that give the large chirality flipping enhancement from muon $g-2$ i.e., y_R^{μ} and $y_L^{b\mu}$ are non-vanishing in the new Yukawa coupling,

with

$$F(m_1, m_2) = m_1^2 + m_2^2 - \frac{2m_1^2 m_2^2}{m_1^2 - m_2^2} \log\left(\frac{m_1^2}{m_2^2}\right). \quad (13)$$

This function vanishes when the masses are degenerate, that is, $\lim_{m_1 \rightarrow m_2} F(m_1, m_2) = 0$. When $\Delta m = 0$, the custodial symmetry is restored, and the corrections to the T parameter vanish as $m_{S_3} = m_+ = m_-$. The shift in M_W from the SM prediction can be related to the oblique T parameter via,

$$\Delta M_W^2 \equiv M_W^2|_{\text{BSM}} - M_W^2|_{\text{SM}} = \frac{\alpha c_W^4 M_Z^2}{c_W^2 - s_W^2} T \quad (14)$$

After EW symmetry breaking, we have four scalar LQs, one with an electromagnetic charge $Q = 4/3$, one with $Q = -2/3$ and two with $Q = 1/3$. The $Q = 1/3$ states mix through the λ interaction resulting in mass eigenstates $S_+^{\pm 1/3}$ and $S_-^{\pm 1/3}$ with masses m_{S_+} and m_{S_-} :

$$\begin{pmatrix} S_+^{\pm 1/3} \\ S_-^{\pm 1/3} \end{pmatrix} = \begin{pmatrix} c_\phi & s_\phi \\ -s_\phi & c_\phi \end{pmatrix} \begin{pmatrix} S_+^{\pm 1/3} \\ S_-^{\pm 1/3} \end{pmatrix}. \quad (8)$$

where ϕ is the mixing angle. The masses m_{S_3} , m_{S_1} and the mixing parameter λ can be obtained from m_{S_+} , m_{S_-} and ϕ from

$$\delta = \frac{\lambda v^2}{2} = s_\phi c_\phi (m_{S_-}^2 - m_{S_+}^2) \quad (9)$$

$$m_{S_1}^2 = m_{S_+}^2 c_\phi^2 + m_{S_-}^2 s_\phi^2 \quad (10)$$

$$m_{S_3}^2 = m_{S_+}^2 s_\phi^2 + m_{S_-}^2 c_\phi^2 \quad (11)$$

where $v = 246$ GeV is the vacuum expectation value. We also define $\Delta m \equiv m_{S_-} - m_{S_+}$ as the mass splitting between the two mass eigenstates S_+ and S_- . This mass splitting generates a non-vanishing oblique correction to the T parameter at one-loop [97],

$$T = \frac{3}{4\pi s_W^2} \frac{1}{M_W^2} \left[F(m_{S_3}, m_{S_-}) \cos^2 \phi + F(m_{S_3}, m_{S_+}) \sin^2 \phi \right] \quad (12)$$

where c_W and s_W are the cosine and sine of the Weinberg angle. There are, furthermore, contributions from S and U that are subdominant in our LQ model. We determine the T that is required to explain the CDF 2022 measurement from our EW global fits and use that in combination with eq. (12) to test if LQ scenarios can explain this data. We checked analytically and numerically that our calculation obeys decoupling, with the additional BSM contributions approaching zero in the limit of large LQ masses. We cross-checked eq. (12) with a full one-loop calculation of the T parameter using SARAH 4.14.3 [98], FeynArts 3.11 [99], FormCalc 9.9 [100] and LoopTools 2.16 [101], finding good agreement with the results using just eq. (12). With the same setup we also verified that the combined contributions from S and U to M_W are small and do not impact significantly on our results. Finally we also implemented this model in FlexibleSUSY [102–105] using the same SARAH model file and the recently updated M_W calculation [105] and again found reasonable agreement with the results of our analysis described above.

Whilst the mass splitting impacts the W mass, the mixing impacts muon $g-2$. Indeed, the mixing between interaction eigenstates allows the physical mass eigenstates to have both left- and right-handed couplings to muons and induces chirality flipping enhancements to muon $g-2$ [97]

$$\delta a_\mu = -\frac{3m_\mu^2}{16\pi^2} \frac{m_t}{m_\mu} \sin 2\phi y_{LYR} \left(\frac{G(x_t^+)}{m_{S_+}^2} - \frac{G(x_t^-)}{m_{S_-}^2} \right) \quad (15)$$

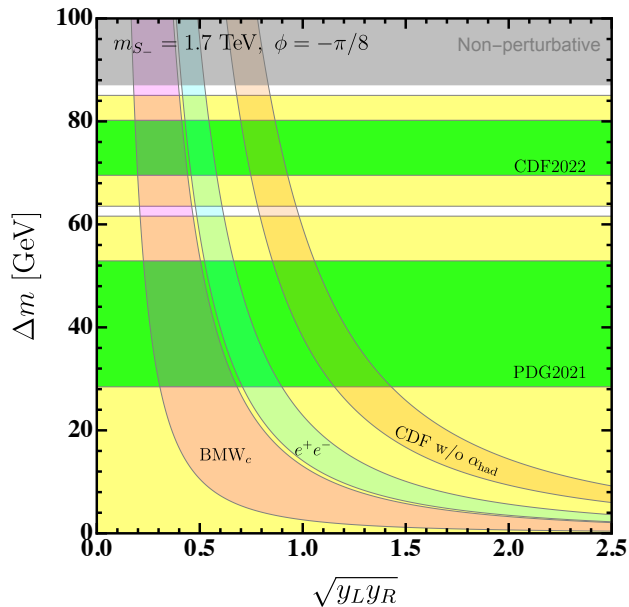


Figure 3. **Scalar leptoquark explanation.** Regions in the Δm – $\sqrt{y_L y_R}$ plane of our LQ model that predict the W -boson mass and muon $g - 2$ in agreement with measurements. The mixing angle ϕ is set to be $-\pi/8$ and $m_{S_-} = 1.7$ TeV. The gray region is excluded by the perturbativity requirement $|\lambda| < \sqrt{4\pi}$.

where $x_i^\pm = m_i^2/m_{S_\pm}^2$, the loop function is $G(x) = 1/3g_S(x) - g_F(x)$ with

$$\begin{aligned} g_S(x) &= \frac{1}{x-1} - \frac{\log x}{(x-1)^2} \\ g_F(x) &= \frac{x-3}{2(x-1)^2} + \frac{\log x}{(x-1)^3}, \end{aligned} \quad (16)$$

and we simplify our notation by letting $y_L \equiv y_L^{b\mu}$ and $y_R \equiv y_R^{l\mu}$. Note that in this case there is a cancellation between the contribution of the lighter and heavier mass eigenstates, which reduces the effect of the very large chirality flipping enhancement m_i/m_μ somewhat. If we consider couplings between S_1 state and left-handed muons as well, the contributions would be considerably enhanced, so this would simply make it easier to explain a_μ while having little or no impact on the W mass prediction.

BSM contributions to a_μ and the W mass both require non-vanishing Δm . For a_μ , it further requires non-vanishing mixing ϕ and relies on $y_L y_R$. Thus it is possible to find explanations of both a_μ and the 2022 CDF measurement of M_W by varying $y_L y_R$ and Δm with non-zero mixing angle ϕ . In fig. 3 we show regions in the Δm – $\sqrt{y_L y_R}$ plane that explain both measurements, where we have fixed the LQ mass to 1.7 TeV, a little above the LHC limit, and we also fixed the mixing angle $\phi = -\pi/8$.

LQ couplings of greater than about a half can explain the a_μ measurement within 1σ when we use the SM prediction from the theory white paper, where e^+e^- data is used for a_μ^{HVP} . Ex-

plaining the SM prediction from the BMW collaboration requires even smaller couplings, though in this case the tension with the SM is anyway less than 2σ . Using e^+e^- data to also fix $\Delta\alpha_{\text{had}}$ means there then remains an additional deviation between the SM M_W prediction and the measured values. To explain the new 2022 CDF result with BSM contributions as well, $\Delta m \approx 75$ GeV is then required, and the dual explanation of the M_W and a_μ anomalies can be achieved in the region where the green CDF 2022 band overlaps with the light blue e^+e^- band in fig. 3. The deviation between the SM prediction for the W boson mass and the 2021 PDG value is not so large and within 2σ it does not need new physics contributions, so the yellow 2σ band for this in fig. 3 can extend to $\Delta m \approx 0$, but to within 1σ a small non-zero Δm is required. Further, the interaction coupling λ is proportional to the mass splitting Δm with fixed mixing angle ϕ . In order to keep the coupling perturbative ($|\lambda| < \sqrt{4\pi}$), there is an upper limit on the mass splitting as shown by the grey band in fig. 3. Note that the region that can accommodate the CDF measurement is close to the non-perturbative region, as the CDF measurement requires large mass splitting. However, it is still possible to explain the new M_W measurement within 1σ in the perturbative region.

Further constraints

This model establishes a proof of principle of a simple, dual explanation of both anomalies. There remains, however, the question of whether this model or extensions of it can simultaneously explain recent flavour physics measurements and anomalies and satisfy additional phenomenological constraints. The latter may be particularly severe as the required Yukawa couplings are $\mathcal{O}(1)$.

For example, the recently measured branching ratio $\text{BR}(h \rightarrow \mu\mu)$ [106, 107] can be an important probe of leptoquark explanations of muon $g - 2$ [108, 109]. Ref. [108] showed that when you have S_1 and S_3 with only right-handed couplings for S_1 there is already a significant tension with the current measurements. There are several ways to avoid this tension. If the leptoquarks are embedded in a more fundamental theory there could be additional light states that result in cancellations with the leptoquark contribution to $h \rightarrow \mu\mu$, for example through destructive interference between tree- and loop-level diagrams. This can be achieved by extending the LQ model in the framework of the two-Higgs-doublet model in the wrong-sign Yukawa coupling region [110]. Alternatively we can reintroduce the left-handed coupling of the S_1 state, which brings two benefits.

First, allowing significant left-handed couplings from S_1 substantially reduces the size of the Yukawa couplings needed to explain muon $g - 2$ (as stated earlier). We show in the Supplementary Note 3 that, as can be anticipated from Ref. [108], this makes it possible to satisfy the $\text{BR}(h \rightarrow \mu\mu)$ data while simultaneously explaining muon $g - 2$, while keeping the mass splitting fixed to a value required to explain the CDF measurement of the W mass. Second introducing this cou-

pling gives additional freedom that can help explain the well-known anomalies of Lepton Flavour Universality Violation, while avoiding other limits from flavour physics.

Indeed, the severe constraints from $\mu \rightarrow e\gamma$, a_e , etc. can all be evaded by allowing the proper flavour ansatz for the Yukawa couplings [111]. At the same time the R_{K^*} and R_{D^*} anomalies can be explained via extra tree-level processes from the scalar LQ with $Q = 4/3$ to $b \rightarrow s\mu^+\mu^-$ and two scalar LQs with $Q = 1/3$ to $b \rightarrow c\tau\nu$. Although the latter two scalar LQs also contribute to $R_{K^*}^{\nu}$ through tree-level process $b \rightarrow s\nu\nu$, these enhancements are under control and their effects are not in conflict with the current measurement [111].

Finally, we show that an explanation of the W mass in our model must be accompanied by new physics below about 2 TeV. In order to explain the CDF measurement at 2σ with $S = 0$ (which is a good approximation in our model), we need $0.14 \lesssim T \lesssim 0.17$. Expanding eq. (12),

$$T \simeq \frac{\lambda^2 v^4}{16\pi m_-^2 M_W^2 s_W^2} \quad (17)$$

such that combining the lower limit on the T parameter and the perturbativity limit $\lambda \leq \sqrt{4\pi}$ we obtain

$$m_- \lesssim 2 \text{ TeV} \quad (18)$$

As the mass splitting, $\Delta m = m_+ - m_- \lesssim 100 \text{ GeV}$, our model thus predicts two $Q = 1/3$ LQ states below about 2 TeV.

DATA AVAILABILITY

The datasets generated during and/or analysed during the current study are available from the corresponding author on request.

CODE AVAILABILITY

The custom computer codes used to generate results are available from the corresponding author on request.

REFERENCES

-
- [1] Aaltonen, T. *et al.* High-precision measurement of the W boson mass with the CDF II detector. *Science* **376**, 170–176 (2022).
- [2] Abi, B. *et al.* Measurement of the Positive Muon Anomalous Magnetic Moment to 0.46 ppm. *Phys. Rev. Lett.* **126**, 141801 (2021). 2104.03281.
- [3] Aoyama, T. *et al.* The anomalous magnetic moment of the muon in the Standard Model. *Phys. Rept.* **887**, 1–166 (2020). 2006.04822.
- [4] Aoyama, T., Hayakawa, M., Kinoshita, T. & Nio, M. Complete Tenth-Order QED Contribution to the Muon $g - 2$. *Phys. Rev. Lett.* **109**, 111808 (2012). 1205.5370.
- [5] Aoyama, T., Kinoshita, T. & Nio, M. Theory of the Anomalous Magnetic Moment of the Electron. *Atoms* **7**, 28 (2019).
- [6] Czarnecki, A., Marciano, W. J. & Vainshtein, A. Refinements in electroweak contributions to the muon anomalous magnetic moment. *Phys. Rev.* **D67**, 073006 (2003). [Erratum: *Phys. Rev.* **D73**, 119901 (2006)], hep-ph/0212229.
- [7] Gnendiger, C., Stöckinger, D. & Stöckinger-Kim, H. The electroweak contributions to $(g - 2)_\mu$ after the Higgs boson mass measurement. *Phys. Rev.* **D88**, 053005 (2013). 1306.5546.
- [8] Davier, M., Hoecker, A., Malaescu, B. & Zhang, Z. Reevaluation of the hadronic vacuum polarisation contributions to the Standard Model predictions of the muon $g - 2$ and $\alpha(M_Z^2)$ using newest hadronic cross-section data. *Eur. Phys. J. C* **77**, 827 (2017). 1706.09436.
- [9] Keshavarzi, A., Nomura, D. & Teubner, T. Muon $g - 2$ and $\alpha(M_Z^2)$: a new data-based analysis. *Phys. Rev. D* **97**, 114025 (2018). 1802.02995.
- [10] Colangelo, G., Hoferichter, M. & Stoffer, P. Two-pion contribution to hadronic vacuum polarization. *JHEP* **02**, 006 (2019). 1810.00007.
- [11] Hoferichter, M., Hoid, B.-L. & Kubis, B. Three-pion contribution to hadronic vacuum polarization. *JHEP* **08**, 137 (2019). 1907.01556.
- [12] Davier, M., Hoecker, A., Malaescu, B. & Zhang, Z. A new evaluation of the hadronic vacuum polarisation contributions to the muon anomalous magnetic moment and to $\alpha(m_Z^2)$. *Eur. Phys. J. C* **80**, 241 (2020). [Erratum: *Eur. Phys. J. C* **80**, 410 (2020)], 1908.00921.
- [13] Keshavarzi, A., Nomura, D. & Teubner, T. $g - 2$ of charged leptons, $\alpha(M_Z^2)$, and the hyperfine splitting of muonium. *Phys. Rev. D* **101**, 014029 (2020). 1911.00367.
- [14] Kurz, A., Liu, T., Marquard, P. & Steinhauser, M. Hadronic contribution to the muon anomalous magnetic moment to next-to-next-to-leading order. *Phys. Lett.* **B734**, 144–147 (2014). 1403.6400.
- [15] Melnikov, K. & Vainshtein, A. Hadronic light-by-light scattering contribution to the muon anomalous magnetic moment revisited. *Phys. Rev.* **D70**, 113006 (2004). hep-ph/0312226.
- [16] Masjuan, P. & Sánchez-Puertas, P. Pseudoscalar-pole contribution to the $(g_\mu - 2)$: a rational approach. *Phys. Rev.* **D95**, 054026 (2017). 1701.05829.
- [17] Colangelo, G., Hoferichter, M., Procura, M. & Stoffer, P. Dispersion relation for hadronic light-by-light scattering: two-pion contributions. *JHEP* **04**, 161 (2017). 1702.07347.
- [18] Hoferichter, M., Hoid, B.-L., Kubis, B., Leupold, S. & Schneider, S. P. Dispersion relation for hadronic light-by-light scattering: pion pole. *JHEP* **10**, 141 (2018). 1808.04823.
- [19] Gérardin, A., Meyer, H. B. & Nyffeler, A. Lattice calculation of the pion transition form factor with $N_f = 2 + 1$ Wilson quarks. *Phys. Rev.* **D100**, 034520 (2019). 1903.09471.
- [20] Bijmans, J., Hermansson-Truedsson, N. & Rodríguez-Sánchez, A. Short-distance constraints for the HLbL contribution to the muon anomalous magnetic moment. *Phys. Lett.* **B798**, 134994 (2019). 1908.03331.
- [21] Colangelo, G., Hagelstein, F., Hoferichter, M., Laub, L. & Stoffer, P. Longitudinal short-distance constraints for the hadronic light-by-light contribution to $(g - 2)_\mu$ with large- N_c Regge models. *JHEP* **03**, 101 (2020). 1910.13432.
- [22] Pauk, V. & Vanderhaeghen, M. Single meson contributions to the muon's anomalous magnetic moment. *Eur. Phys. J. C* **74**, 3008 (2014). 1401.0832.

- [23] Danilkin, I. & Vanderhaeghen, M. Light-by-light scattering sum rules in light of new data. *Phys. Rev.* **D95**, 014019 (2017). 1611.04646.
- [24] Jegerlehner, F. The Anomalous Magnetic Moment of the Muon. *Springer Tracts Mod. Phys.* **274**, 1–693 (2017).
- [25] Knecht, M., Narison, S., Rabemananjara, A. & Rabetiarivony, D. Scalar meson contributions to a_μ from hadronic light-by-light scattering. *Phys. Lett.* **B787**, 111–123 (2018). 1808.03848.
- [26] Eichmann, G., Fischer, C. S. & Williams, R. Kaon-box contribution to the anomalous magnetic moment of the muon. *Phys. Rev.* **D101**, 054015 (2020). 1910.06795.
- [27] Roig, P. & Sánchez-Puertas, P. Axial-vector exchange contribution to the hadronic light-by-light piece of the muon anomalous magnetic moment. *Phys. Rev.* **D101**, 074019 (2020). 1910.02881.
- [28] Blum, T. *et al.* The hadronic light-by-light scattering contribution to the muon anomalous magnetic moment from lattice QCD. *Phys. Rev. Lett.* **124**, 132002 (2020). 1911.08123.
- [29] Colangelo, G., Hoferichter, M., Nyffeler, A., Passera, M. & Stoffer, P. Remarks on higher-order hadronic corrections to the muon $g - 2$. *Phys. Lett.* **B735**, 90–91 (2014). 1403.7512.
- [30] Bennett, G. W. *et al.* Final Report of the Muon E821 Anomalous Magnetic Moment Measurement at BNL. *Phys. Rev. D* **73**, 072003 (2006). hep-ex/0602035.
- [31] Aaltonen, T. *et al.* Precise measurement of the W -boson mass with the CDF II detector. *Phys. Rev. Lett.* **108**, 151803 (2012). 1203.0275.
- [32] Schael, S. *et al.* Electroweak Measurements in Electron-Positron Collisions at W -Boson-Pair Energies at LEP. *Phys. Rept.* **532**, 119–244 (2013). 1302.3415.
- [33] Aaij, R. *et al.* Measurement of the W boson mass. *JHEP* **01**, 036 (2022). 2109.01113.
- [34] Aaboud, M. *et al.* Measurement of the W -boson mass in pp collisions at $\sqrt{s} = 7$ TeV with the ATLAS detector. *Eur. Phys. J. C* **78**, 110 (2018). [Erratum: *Eur. Phys. J. C* **78**, 898 (2018)], 1701.07240.
- [35] Abazov, V. M. *et al.* Measurement of the W Boson Mass with the D0 Detector. *Phys. Rev. Lett.* **108**, 151804 (2012). 1203.0293.
- [36] Aaltonen, T. A. *et al.* Combination of CDF and D0 W -Boson Mass Measurements. *Phys. Rev. D* **88**, 052018 (2013). 1307.7627.
- [37] Haller, J. *et al.* Update of the global electroweak fit and constraints on two-Higgs-doublet models. *Eur. Phys. J. C* **78**, 675 (2018). 1803.01853.
- [38] Zyla, P. *et al.* Review of Particle Physics. *PTEP* **2020**, 083C01 (2020).
- [39] Athron, P. *et al.* GitHub repository — W mass combination. https://github.com/andrewfowlie/w_mass_combination.
- [40] Awramik, M., Czakon, M., Freitas, A. & Weiglein, G. Precise prediction for the W boson mass in the standard model. *Phys. Rev. D* **69**, 053006 (2004). hep-ph/0311148.
- [41] Sirlin, A. Radiative Corrections in the $SU(2)_L \times U(1)$ Theory: A Simple Renormalization Framework. *Phys. Rev. D* **22**, 971–981 (1980).
- [42] Marciano, W. J. & Sirlin, A. Radiative Corrections to Neutrino Induced Neutral Current Phenomena in the $SU(2)_L \times U(1)$ Theory. *Phys. Rev. D* **22**, 2695 (1980). [Erratum: *Phys. Rev.* **D31**, 213 (1985)].
- [43] Sirlin, A. On the $O(\alpha_s^2)$ Corrections to τ (μ), $m(W)$, $m(Z)$ in the $SU(2)_L \times U(1)$ Theory. *Phys. Rev. D* **29**, 89 (1984).
- [44] Djouadi, A. & Verzegnassi, C. Virtual Very Heavy Top Effects in LEP / SLC Precision Measurements. *Phys. Lett. B* **195**, 265–271 (1987).
- [45] Djouadi, A. $O(\alpha_s)$ Vacuum Polarization Functions of the Standard Model Gauge Bosons. *Nuovo Cim. A* **100**, 357 (1988).
- [46] Kniehl, B. A. Two Loop Corrections to the Vacuum Polarizations in Perturbative QCD. *Nucl. Phys. B* **347**, 86–104 (1990).
- [47] Consoli, M., Hollik, W. & Jegerlehner, F. The Effect of the Top Quark on the $M(W)$ - $M(Z)$ Interdependence and Possible Decoupling of Heavy Fermions from Low-Energy Physics. *Phys. Lett. B* **227**, 167–170 (1989).
- [48] Halzen, F. & Kniehl, B. A. Δr beyond one loop. *Nucl. Phys. B* **353**, 567–590 (1991).
- [49] Kniehl, B. A. & Sirlin, A. Dispersion relations for vacuum polarization functions in electroweak physics. *Nucl. Phys. B* **371**, 141–148 (1992).
- [50] Barbieri, R., Beccaria, M., Ciafaloni, P., Curci, G. & Vicere, A. Radiative correction effects of a very heavy top. *Phys. Lett. B* **288**, 95–98 (1992). [Erratum: *Phys. Lett. B* **312**, 511–511 (1993)], hep-ph/9205238.
- [51] Djouadi, A. & Gambino, P. Electroweak gauge bosons self-energies: Complete QCD corrections. *Phys. Rev. D* **49**, 3499–3511 (1994). [Erratum: *Phys. Rev.* **D53**, 4111 (1996)], hep-ph/9309298.
- [52] Fleischer, J., Tarasov, O. V. & Jegerlehner, F. Two loop heavy top corrections to the rho parameter: A Simple formula valid for arbitrary Higgs mass. *Phys. Lett. B* **319**, 249–256 (1993).
- [53] Degrassi, G., Gambino, P. & Vicini, A. Two loop heavy top effects on the $m(Z) - m(W)$ interdependence. *Phys. Lett. B* **383**, 219–226 (1996). hep-ph/9603374.
- [54] Degrassi, G., Gambino, P. & Sirlin, A. Precise calculation of $M(W)$, $\sin^2 \theta(W)$ ($M(Z)$), and $\sin^2 \theta(\text{eff})(\text{lept})$. *Phys. Lett. B* **394**, 188–194 (1997). hep-ph/9611363.
- [55] Freitas, A., Hollik, W., Walter, W. & Weiglein, G. Complete fermionic two loop results for the $M(W) - M(Z)$ interdependence. *Phys. Lett. B* **495**, 338–346 (2000). [Erratum: *Phys. Lett. B* **570**, 265 (2003)], hep-ph/0007091.
- [56] Freitas, A., Hollik, W., Walter, W. & Weiglein, G. Electroweak two loop corrections to the $M_W - M_Z$ mass correlation in the standard model. *Nucl. Phys. B* **632**, 189–218 (2002). [Erratum: *Nucl. Phys. B* **666**, 305–307 (2003)], hep-ph/0202131.
- [57] Awramik, M. & Czakon, M. Complete two loop bosonic contributions to the muon lifetime in the standard model. *Phys. Rev. Lett.* **89**, 241801 (2002). hep-ph/0208113.
- [58] Awramik, M. & Czakon, M. Complete two loop electroweak contributions to the muon lifetime in the standard model. *Phys. Lett. B* **568**, 48–54 (2003). hep-ph/0305248.
- [59] Onishchenko, A. & Veretin, O. Two loop bosonic electroweak corrections to the muon lifetime and $M(Z) - M(W)$ interdependence. *Phys. Lett. B* **551**, 111–114 (2003). hep-ph/0209010.
- [60] Awramik, M., Czakon, M., Onishchenko, A. & Veretin, O. Bosonic corrections to Δr at the two loop level. *Phys. Rev. D* **68**, 053004 (2003). hep-ph/0209084.
- [61] Avdeev, L., Fleischer, J., Mikhailov, S. & Tarasov, O. $O(\alpha_s^2)$ correction to the electroweak ρ parameter. *Phys. Lett. B* **336**, 560–566 (1994). [Erratum: *Phys. Lett. B* **349**, 597–598 (1995)], hep-ph/9406363.
- [62] Chetyrkin, K. G., Kuhn, J. H. & Steinhauser, M. Corrections of order $O(G_F M_t^2 \alpha_s^2)$ to the ρ parameter. *Phys. Lett. B* **351**, 331–338 (1995). hep-ph/9502291.
- [63] Chetyrkin, K. G., Kuhn, J. H. & Steinhauser, M. QCD corrections from top quark to relations between electroweak parameters to order α_s^2 . *Phys. Rev. Lett.* **75**, 3394–3397

- (1995). hep-ph/9504413.
- [64] Chetyrkin, K. G., Kuhn, J. H. & Steinhauser, M. Three loop polarization function and $O(\alpha_s^2)$ corrections to the production of heavy quarks. *Nucl. Phys. B* **482**, 213–240 (1996). hep-ph/9606230.
- [65] Faisst, M., Kuhn, J. H., Seidensticker, T. & Veretin, O. Three loop top quark contributions to the rho parameter. *Nucl. Phys. B* **665**, 649–662 (2003). hep-ph/0302275.
- [66] van der Bij, J. J., Chetyrkin, K. G., Faisst, M., Jikia, G. & Seidensticker, T. Three loop leading top mass contributions to the rho parameter. *Phys. Lett. B* **498**, 156–162 (2001). hep-ph/0011373.
- [67] Boughezal, R., Tausk, J. B. & van der Bij, J. J. Three-loop electroweak correction to the Rho parameter in the large Higgs mass limit. *Nucl. Phys. B* **713**, 278–290 (2005). hep-ph/0410216.
- [68] Boughezal, R. & Czakon, M. Single scale tadpoles and $O(G_F m(t)^2 \alpha_s^3)$ corrections to the rho parameter. *Nucl. Phys. B* **755**, 221–238 (2006). hep-ph/0606232.
- [69] Chetyrkin, K. G., Faisst, M., Kuhn, J. H., Maierhofer, P. & Sturm, C. Four-Loop QCD Corrections to the Rho Parameter. *Phys. Rev. Lett.* **97**, 102003 (2006). hep-ph/0605201.
- [70] Schroder, Y. & Steinhauser, M. Four-loop singlet contribution to the rho parameter. *Phys. Lett. B* **622**, 124–130 (2005). hep-ph/0504055.
- [71] Diessner, P. & Weiglein, G. Precise prediction for the W boson mass in the MRSSM. *JHEP* **07**, 011 (2019). 1904.03634.
- [72] Degrassi, G., Gambino, P. & Giardino, P. P. The $m_W - m_Z$ interdependence in the Standard Model: a new scrutiny. *JHEP* **05**, 154 (2015). 1411.7040.
- [73] Crivellin, A., Hoferichter, M., Manzari, C. A. & Montull, M. Hadronic Vacuum Polarization: $(g - 2)_\mu$ versus Global Electroweak Fits. *Phys. Rev. Lett.* **125**, 091801 (2020). 2003.04886.
- [74] de Blas, J. *et al.* Global analysis of electroweak data in the Standard Model (2021). 2112.07274.
- [75] Lautrup, B. E. & De Rafael, E. Calculation of the sixth-order contribution from the fourth-order vacuum polarization to the difference of the anomalous magnetic moments of muon and electron. *Phys. Rev.* **174**, 1835–1842 (1968).
- [76] Achasov, N. N. & Kiselev, A. V. Contribution to muon $g-2$ from the π^0 gamma and eta gamma intermediate states in the vacuum polarization. *Phys. Rev. D* **65**, 097302 (2002). hep-ph/0202047.
- [77] Hoferichter, M., Hoid, B.-L. & Kubis, B. Three-pion contribution to hadronic vacuum polarization. *JHEP* **08**, 137 (2019). 1907.01556.
- [78] Borsanyi, S. *et al.* Leading hadronic contribution to the muon magnetic moment from lattice QCD. *Nature* **593**, 51–55 (2021). 2002.12347.
- [79] Passera, M., Marciano, W. J. & Sirlin, A. The Muon $g-2$ and the bounds on the Higgs boson mass. *Phys. Rev. D* **78**, 013009 (2008). 0804.1142.
- [80] Keshavarzi, A., Marciano, W. J., Passera, M. & Sirlin, A. Muon $g - 2$ and $\Delta\alpha$ connection. *Phys. Rev. D* **102**, 033002 (2020). 2006.12666.
- [81] de Rafael, E. Constraints between $\Delta\alpha_{\text{had}}(M_Z^2)$ and $(g_\mu - 2)_{\text{HVP}}$. *Phys. Rev. D* **102**, 056025 (2020). 2006.13880.
- [82] Flacher, H. *et al.* Revisiting the Global Electroweak Fit of the Standard Model and Beyond with Gfit. *Eur. Phys. J. C* **60**, 543–583 (2009). [Erratum: *Eur. Phys. J. C* **71**, 1718 (2011)], 0811.0009.
- [83] Baak, M. *et al.* Updated Status of the Global Electroweak Fit and Constraints on New Physics. *Eur. Phys. J. C* **72**, 2003 (2012). 1107.0975.
- [84] Baak, M. *et al.* The Electroweak Fit of the Standard Model after the Discovery of a New Boson at the LHC. *Eur. Phys. J. C* **72**, 2205 (2012). 1209.2716.
- [85] Baak, M. *et al.* The global electroweak fit at NNLO and prospects for the LHC and ILC. *Eur. Phys. J. C* **74**, 3046 (2014). 1407.3792.
- [86] Zyla, P. A. *et al.* Review of Particle Physics. *PTEP* **2020**, 083C01 (2020).
- [87] Stockinger, D. The Muon Magnetic Moment and Supersymmetry. *J. Phys. G* **34**, R45–R92 (2007). hep-ph/0609168.
- [88] Athron, P. *et al.* New physics explanations of a_μ in light of the FNAL muon $g - 2$ measurement. *JHEP* **09**, 080 (2021). 2104.03691.
- [89] Peskin, M. E. & Takeuchi, T. Estimation of oblique electroweak corrections. *Phys. Rev. D* **46**, 381–409 (1992).
- [90] Cacciapaglia, G. & Sannino, F. The W boson mass weighs in on the non-standard Higgs (2022). 2204.04514.
- [91] Doršner, I., Fajfer, S., Greljo, A., Kamenik, J. F. & Košnik, N. Physics of leptoquarks in precision experiments and at particle colliders. *Phys. Rept.* **641**, 1–68 (2016). 1603.04993.
- [92] Buchmuller, W., Ruckl, R. & Wyler, D. Leptoquarks in Lepton - Quark Collisions. *Phys. Lett. B* **191**, 442–448 (1987). [Erratum: *Phys. Lett. B* **448**, 320–320 (1999)].
- [93] Choi, S.-M., Kang, Y.-J., Lee, H. M. & Ro, T.-G. Lepto-Quark Portal Dark Matter. *JHEP* **10**, 104 (2018). 1807.06547.
- [94] Lee, H. M. Leptoquark option for B-meson anomalies and leptonic signatures. *Phys. Rev. D* **104**, 015007 (2021). 2104.02982.
- [95] Chakraverty, D., Choudhury, D. & Datta, A. A Nonsupersymmetric resolution of the anomalous muon magnetic moment. *Phys. Lett. B* **506**, 103–108 (2001). hep-ph/0102180.
- [96] Bauer, M. & Neubert, M. Minimal leptoquark explanation for the $R_{D^{(*)}}$, R_K , and $(g - 2)_\mu$ anomalies. *Phys. Rev. Lett.* **116**, 141802 (2016). URL <https://link.aps.org/doi/10.1103/PhysRevLett.116.141802>.
- [97] Doršner, I., Fajfer, S. & Sumensari, O. Muon $g - 2$ and scalar leptoquark mixing. *JHEP* **06**, 089 (2020). 1910.03877.
- [98] Staub, F. SARAH 4 : A tool for (not only SUSY) model builders. *Comput. Phys. Commun.* **185**, 1773–1790 (2014). 1309.7223.
- [99] Hahn, T. Generating Feynman diagrams and amplitudes with FeynArts 3. *Comput. Phys. Commun.* **140**, 418–431 (2001). hep-ph/0012260.
- [100] Hahn, T., Paßehr, S. & Schappacher, C. FormCalc 9 and Extensions. *PoS LL2016*, 068 (2016). 1604.04611.
- [101] Hahn, T. & Perez-Victoria, M. Automatized one loop calculations in four-dimensions and D-dimensions. *Comput. Phys. Commun.* **118**, 153–165 (1999). hep-ph/9807565.
- [102] Athron, P., Park, J.-h., Stöckinger, D. & Voigt, A. FlexibleSUSY—A spectrum generator generator for supersymmetric models. *Comput. Phys. Commun.* **190**, 139–172 (2015). 1406.2319.
- [103] Athron, P. *et al.* FlexibleSUSY 2.0: Extensions to investigate the phenomenology of SUSY and non-SUSY models. *Comput. Phys. Commun.* **230**, 145–217 (2018). 1710.03760.
- [104] Athron, P. *et al.* FlexibleDecay: An automated calculator of scalar decay widths (2021). 2106.05038.
- [105] Athron, P. *et al.* Precise calculation of the W boson pole mass beyond the Standard Model with FlexibleSUSY (2022). 2204.05285.
- [106] Aad, G. *et al.* A search for the dimuon decay of the Standard Model Higgs boson with the ATLAS detector. *Phys. Lett. B* **812**, 135980 (2021). 2007.07830.

- [107] Sirunyan, A. M. *et al.* Evidence for Higgs boson decay to a pair of muons. *JHEP* **01**, 148 (2021). 2009.04363.
- [108] Crivellin, A., Mueller, D. & Saturnino, F. Correlating $h \rightarrow \mu + \mu^-$ to the Anomalous Magnetic Moment of the Muon via Leptoquarks. *Phys. Rev. Lett.* **127**, 021801 (2021). 2008.02643.
- [109] Dermisek, R., Hermanek, K., McGinnis, N. & Yoon, S. The Ellipse of Muon Dipole Moments (2022). 2205.14243.
- [110] Su, W. Probing loop effects in wrong-sign Yukawa coupling region of Type-II 2HDM. *Eur. Phys. J. C* **81**, 404 (2021). 1910.06269.
- [111] Bhaskar, A., Madathil, A. A., Mandal, T. & Mitra, S. Combined explanation of W -mass, muon $g - 2$, $R_{K^{(*)}}$ and $R_{D^{(*)}}$ anomalies in a singlet-triplet scalar leptoquark model (2022). 2204.09031.
- [112] Youden, W. J. Enduring values. *Technometrics* **14**, 1–11 (1972).
- [113] Taylor, B. N. Numerical Comparisons of Several Algorithms for Treating Inconsistent Data in a Least-Squares Adjustment of the Fundamental Constants (1982). URL <https://nvlpubs.nist.gov/nistpubs/Legacy/IR/nbsir81-2426.pdf>.
- [114] Barlow, R. Systematic errors: Facts and fictions. In *Conference on Advanced Statistical Techniques in Particle Physics*, 134–144 (2002). hep-ex/0207026.
- [115] Jeng, M. Bandwagon effects and error bars in particle physics. *Nucl. Instrum. Meth. A* **571**, 704–708 (2007).
- [116] Schael, S. *et al.* Precision electroweak measurements on the Z resonance. *Phys. Rept.* **427**, 257–454 (2006). hep-ex/0509008.
- [117] Aaltonen, T. A. *et al.* Tevatron Run II combination of the effective leptonic electroweak mixing angle. *Phys. Rev. D* **97**, 112007 (2018). 1801.06283.

ACKNOWLEDGMENTS

We thank Martin Hoferichter for his useful comments. PA thanks Dominik Stöckinger for helpful early discussions re-

garding this project. LW and BZ are supported by the National Natural Science Foundation of China (NNSFC) under grants No. 12275134 and 12275232, respectively. PA and AF are supported by the National Natural Science Foundation of China (NNSFC) Research Fund for International Excellent Young Scientists grants 12150610460 and 1950410509, respectively. Y.W. would also like to thank U.S. Department of Energy for the financial support, under grant number DE-SC 0016013.

AUTHOR CONTRIBUTIONS STATEMENT

PA contributed to understanding the connections between muon $g - 2$ and M_W , the scalar leptoquark calculations and constraints, interpreting results and to the writing of all sections of the paper. AF contributed to the introduction, statistical analysis, and interpretation and writing throughout. CL contributed to the original idea, introduction muon $g - 2$ calculation and interpretation as well writing throughout. LW contributed to the introduction, calculations, interpretation, and writing throughout. YW contributed to the electroweak global fits, the calculations in the leptoquark model and writing the corresponding sections. BZ has offered a leptoquark explanation for the newly measured W -mass in CDF and muon $g - 2$ anomaly in Fermi-Lab. He additionally examined correlation between the decay of Higgs bosons into muons and the muon $g - 2$ deviation, where the dangerous constraint is removed by introducing a left-handed contribution.

COMPETING INTERESTS STATEMENT

The authors declare no competing interests.

Supplemental Material: Hadronic Uncertainties versus New Physics for the W boson Mass and Muon $g - 2$ Anomalies

Peter Athron,¹ Andrew Fowlie,¹ Chih-Ting Lu,¹ Lei Wu,¹ Yongcheng Wu,¹ and Bin Zhu,²

¹*Department of Physics and Institute of Theoretical Physics, Nanjing Normal University, Nanjing, 210023, China*

²*Department of Physics, Yantai University, Yantai 264005, China*

In this supplemental material, we present the data in our global fits (Table II), our procedure of our simple combination of M_W and the transformation between $\Delta\alpha_{\text{had}}$ and a_μ^{HVP} .

SUPPLEMENTARY NOTE 1 - SIMPLE COMBINATION OF W MASS MEASUREMENTS

We compute a weighted average of N measurements following a standard procedure (see e.g., Ref. [38]),

$$\bar{x} \pm \Delta x = \frac{\sum_{i=1}^N w_i x_i}{\sum_{i=1}^N w_i} \pm \left(\sum_{i=1}^N w_i \right)^{-1/2} \quad (19)$$

where $w_i = 1/\sigma_i^2$. We include the seven measurements — LEP [32], LHCb [33], ATLAS [34], D0 [35] 92-95 (95/pb) and 02-09 (4.3/fb), CDF [1, 31, 36] 88-95 (107/pb) and 02-11 (9.1/fb) — avoiding double-counting the CDF data. This resulted in our simple combination

$$M_W = 80.411 \pm 0.007 \text{ GeV}. \quad (20)$$

This combination remains about 6σ away from the SM. The chi-squared associated with this estimate,

$$\chi^2 = \sum_{i=1}^N w_i (x_i - \bar{x})^2, \quad (21)$$

was 17.7 with $N - 1 = 6$ degrees of freedom. The associated significance was 2.5σ , found from

$$p = 1 - F_{\chi^2_6}(\chi^2) \quad \text{and} \quad Z = \Phi^{-1}(1 - p) \quad (22)$$

where $F_{\chi^2_n}$ is the chi-squared cumulative density function with n degrees of freedom and Φ is the standard normal cumulative density function. This result depends on the number and choices of measurements combined. The code to reproduce these calculations is available at [GitHub](#).

We note, however, that a true combination should include careful consideration of correlated systematic errors and expert judgment about unstated or underestimated errors and systematics. For example, if the reduced chi-squared indicates discrepant measurements, the PDG [38] may inflate the estimated errors, though this does not impact the central value, or decline to combine them (for further discussion see e.g., Ref. [112–115]). In our case, the PDG prescription would inflate the error by about two, if the measurements were combined. This would reduce the discrepancy with the SM to about 3σ .

SUPPLEMENTARY NOTE 2 - THE RELATIONSHIP BETWEEN $\Delta\alpha_{\text{had}}$ AND a_μ^{HVP}

Since both $\Delta\alpha_{\text{had}}$ and a_μ^{HVP} can be extracted from σ_{had} measurements, changes in σ_{had} affect the transformation between $\Delta\alpha_{\text{had}}$ and a_μ^{HVP} . On the one hand, one can directly use the experimental data from σ_{had} measurements (the e^+e^- data) to derive $\Delta\alpha_{\text{had}}$ and a_μ^{HVP} with the data-driven method as shown in Equation 2 and Equation 3 in the main text. On the other hand, we can extract $\Delta\alpha_{\text{had}}$ from EW fits or from estimates of the HVP contributions from the BMW lattice calculation and use that to indirectly indicate possible changes in σ_{had} compared with the experimental measurements. For the latter, we must make assumptions about the energy dependence of σ_{had} and the energy range in which it changes.

As pointed out in Ref. [73], we could modify σ_{had} only in the energy ranges:

$$m_{\pi_0} \leq \sqrt{s} \leq 1.937 \text{ GeV}, \quad (23)$$

$$m_{\pi_0} \leq \sqrt{s} \leq 11.199 \text{ GeV} \text{ or} \quad (24)$$

$$m_{\pi_0} \leq \sqrt{s} \leq \infty, \quad (25)$$

that is, at low energies, at any moderate energies, or across the entire energy range. The hadronic cross section is unchanged above these thresholds. We previously only considered the latter possibility Equation 25; we now consider Equation 23, Equation 24 and reconsider the relationship between $\Delta\alpha_{\text{had}}$ and a_{μ}^{HVP} , i.e. we follow the procedure introduced in Ref. [73]. We find that using Equation 25 and transforming $\Delta\alpha_{\text{had}}$ to a_{μ}^{HVP} (a_{μ}^{HVP} to $\Delta\alpha_{\text{had}}$) results in the most conservative (aggressive) deviation from the e^+e^- data. However, the low energy range projection Equation 23 shows the opposite behaviour. We assume that σ_{had} changes by an overall factor over the range m_{π_0} to infinity, Equation 25. This is scenario (3) in Ref. [73]. Based on this assumption, we derive a_{μ}^{HVP} from $\Delta\alpha_{\text{had}}$ (and vice-versa) with a naive and uniform scaling of the cross-section from the e^+e^- data [3, 9]. In this way, we obtain alternative predictions for a_{μ}^{HVP} that correspond to the M_W measurement under the assumption that no new physics affects the EW fits.

We use the above method to alter the SM prediction for a_{μ} by taking all contributions except for a_{μ}^{HVP} to be those used in Ref. [3]. We then determine the deviation between the combined 2021 world average and our predictions (δa_{μ}), after combining both theoretical and experimental uncertainties. The experimental uncertainty is fixed to 41×10^{-11} [2], but the theoretical uncertainty depends on the way in which a_{μ}^{HVP} was chosen. Each δa_{μ} is indicated on the right-hand side of Figure 2 in the main text and listed in Table I in the main text where we also show how many standard deviations this represents. Finally, we visualize δa_{μ} and its tension from Table I in the main text in Figure 4.

Lastly, to complete our study of the transformation between $\Delta\alpha_{\text{had}}$ and a_{μ}^{HVP} , we consider case Equation 23. Since the BMW collaboration only released the first two bins data ($0 \text{ GeV} < \sqrt{s} \leq 1 \text{ GeV}$ and $1 \text{ GeV} < \sqrt{s} \leq \sqrt{10} \text{ GeV}$) of $\Delta\alpha_{\text{had}}$ [78], case Equation 23 may be suggested by BMWc results. Therefore, we include this case in Table III for readers as a reference. Note we only use the integral breakdown from Ref. [9, 13] which provided smaller uncertainties for a_{μ}^{HVP} from the e^+e^- data in their calculations. Hence, the δa_{μ} in Table III would be reduced if the integral breakdown from other references [8, 12] was used. A significant caveat to keep in mind is that we don't definitively know whether case Equation 23, Equation 24 or Equation 25 should be preferred.

SUPPLEMENTARY NOTE 3 - THE CORRELATION BETWEEN $\text{BR}(h \rightarrow \mu\mu)$ AND MUON ($g - 2$)

As discussed in Further constraints in the main text, measurements of the branching ratio $\text{BR}(h \rightarrow \mu\mu)$ [106, 107] severely constrain our simplified leptoquark model. Relaxing our simplifications by reintroducing left-handed couplings of the S_1 state, λ_L , substantially reduces the size of the Yukawa couplings needed to explain muon $g - 2$. In Figure 5 we show that this alleviates tension between $g - 2$ and $\text{BR}(h \rightarrow \mu\mu)$. The leptoquark model explains muon $g - 2$ while satisfying experimental upper limits on $\text{BR}(h \rightarrow \mu\mu)$ for $\lambda_L \gtrsim 10^{-2}$. The branching ratio predictions may be SM-like for $\lambda_L \simeq 5 \times 10^{-2}$. Nevertheless, the model typically predicts deviations from the SM-predictions for $\text{BR}(h \rightarrow \mu\mu)$ that may be observable in the future.

SUPPLEMENTARY TABLES

Parameter	Measured value	Ref.
PDG 2021 M_W [GeV]	80.379(12)	[86]
CDF 2022 M_W [GeV]	80.4335(94)	[1]
$\Delta\alpha_{\text{had}}^{(5)}(M_Z^2)$	See text	
m_h [GeV]	125.25(17)	[86]
m_t [GeV] ^a	172.76(58)	[86]
$\alpha_s(M_Z)$	0.1179(9)	[86]
Γ_W [GeV]	2.085(42)	[86]
Γ_Z [GeV]	2.4952(23)	[116]
M_Z [GeV]	91.1875(21)	[116]
$A_{\text{FB}}^{0,b}$	0.0992(16)	[116]
$A_{\text{FB}}^{0,c}$	0.0707(35)	[116]
$A_{\text{FB}}^{0,\ell}$	0.0171	[116]
A_b	0.923(20)	[116]
A_c	0.670(27)	[116]
$A_\ell(\text{SLD})$	0.1513(21)	[116]
$A_\ell(\text{LEP})$	0.1465(33)	[116]
R_b^0	0.21629(66)	[116]
R_c^0	0.1721(30)	[116]
R_ℓ^0	20.767(25)	[116]
σ_h^0 [nb]	41.540(37)	[116]
$\sin^2 \theta_{\text{eff}}^\ell(Q_{\text{FB}})$	0.2324(12)	[116]
$\sin^2 \theta_{\text{eff}}^\ell(\text{Teva})$	0.23148(33)	[117]
\bar{m}_c [GeV]	1.27(2)	[86]
\bar{m}_b [GeV]	4.18 ⁽³⁾ ₍₂₎	[86]

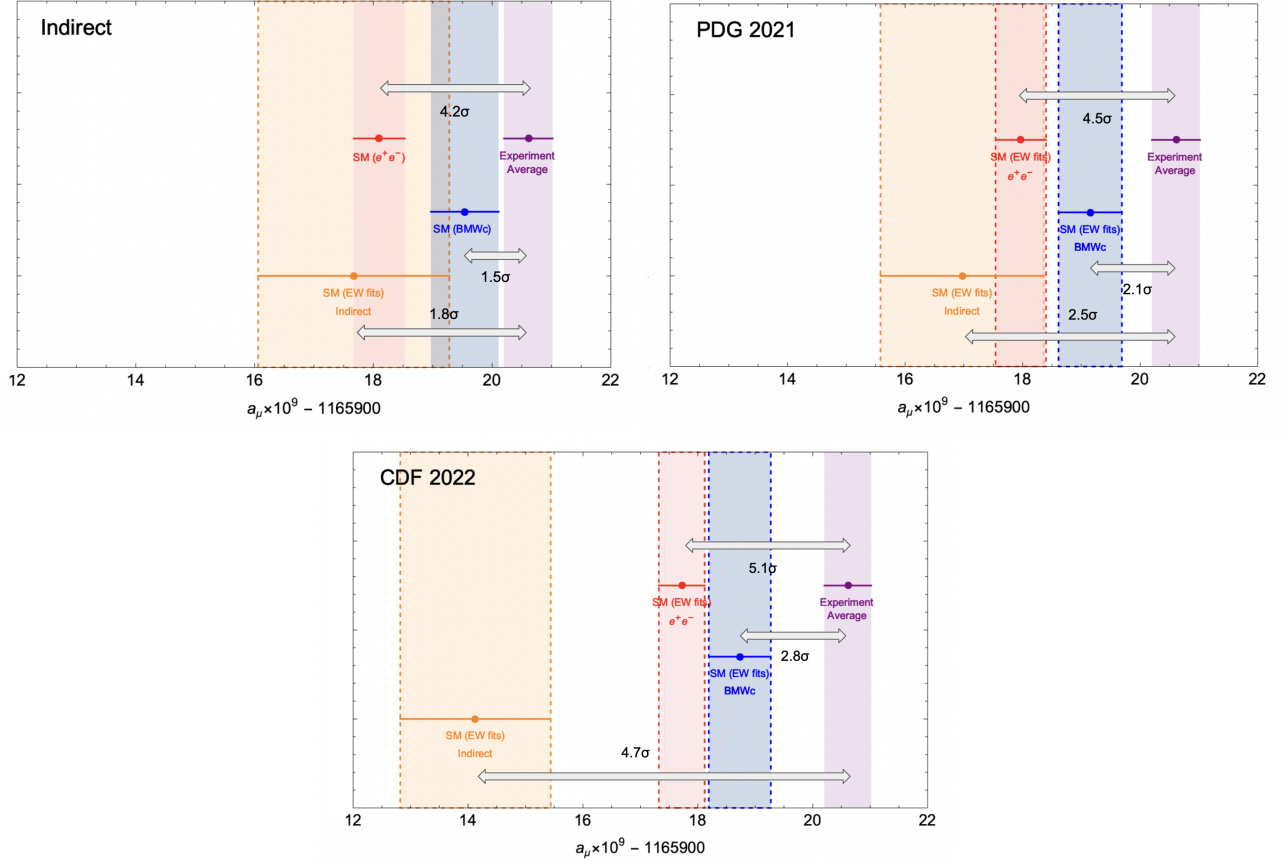
^a 0.5 GeV theoretical uncertainty is included.

Supplementary Table II. The measurements included in the global EW fit. Correlations among $(M_Z, \Gamma_Z, \sigma_h^0, R_\ell^0, A_{\text{FB}}^{0,\ell})$ and among $(A_{\text{FB}}^{0,c}, A_{\text{FB}}^{0,b}, A_c, A_b, R_c^0, R_b^0)$ are also taken into account [116].

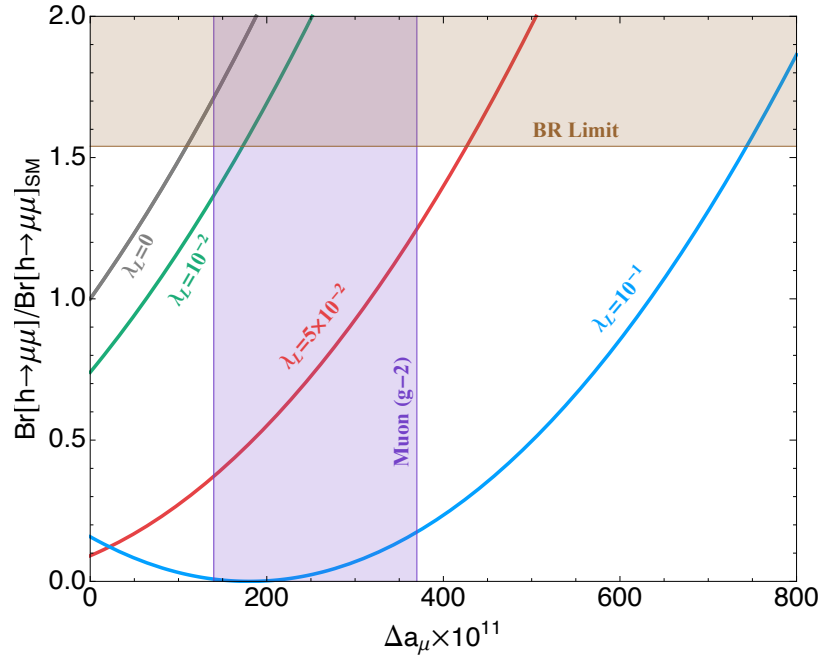
Input	M_W		Indirect		PDG 2021		CDF 2022		Simple Combination		
	$\Delta\alpha_{\text{had}}^{(5)}$	M_W [GeV]	BMWc	e^+e^-	Indirect	BMWc	e^+e^-	Indirect	BMWc	e^+e^-	Indirect
	$\Delta\alpha_{\text{had}}^{(5)}$	M_W [GeV]	-	-	-	80.379(12)	80.379(12)	80.4335(94)	80.4335(94)	80.411(7)	80.411(7)
	$\Delta\alpha_{\text{had}}^{(5)}$	M_W [GeV]	277.4(1.2)	276.1(1.1)	-	277.4(1.2)	276.1(1.1)	276.1(1.1)	276.1(1.1)	277.4(1.2)	276.1(1.1)
	χ^2/dof		16.28/15	16.01/15	15.89/14	19.51/16	18.74/16	62.58/16	47.19/15	52.34/16	49.79/16
	M_W [GeV]		80.355(6)	80.357(6)	80.359(9)	80.360(6)	80.361(6)	80.379(5)	80.396(7)	80.380(5)	80.381(5)
	$\Delta\alpha_{\text{had}} \times 10^4$		277.1(1.2)	275.9(1.1)	274.4(4.4)	276.8(1.1)	275.6(1.1)	274.7(1.0)	260.9(3.6)	275.6(1.1)	274.6(1.0)
Fitted	$\delta a_\mu \times 10^{11}$		-	-	438(396)	173(54)	306(54)	416(54)	1997(320)	306(54)	416(54)
	Tension		-	-	1.1 σ	3.2 σ	5.7 σ	7.7 σ	6.2 σ	5.7 σ	7.7 σ
	δM_W [MeV]		79(11)	77(11)	75(13)	74(11)	73(11)	54(11)	38(12)	54(11)	53(11)
	Tension		7.2 σ	7.0 σ	5.8 σ	6.7 σ	6.6 σ	4.9 σ	3.2 σ	4.9 σ	4.8 σ
											3.7 σ

Supplementary Table III. SM predictions from EW fits for $\Delta\alpha_{\text{had}}$ and M_W , and the differences with respect to measurements of muon $g-2$ and the W mass, δa_μ , and $\delta M_W \equiv M_W^{\text{CDF}} - M_W$ using the low energy projection Equation 23 for the transformation between $\Delta\alpha_{\text{had}}$ and a_μ^{HVP} .

SUPPLEMENTARY FIGURES



Supplementary Figure 4. The a_μ in different fitting scenarios and corresponding tensions with experiment average. The a_μ from experiment average of FNAL E989 and BNL E821 (purple), SM predictions from BMWc (blue), e^+e^- data (red), EW fits w/o $\Delta\alpha_{\text{had}}$ (orange-dashed), EW fits with $\Delta\alpha_{\text{had}}$ from e^+e^- (red-dashed), EW fits with $\Delta\alpha_{\text{had}}$ from BMWc (blue-dashed). The tensions of δa_μ are also shown for the comparison. The upper-left panel is w/o M_W input, the upper-right and bottom panels are with PDG 2021 and CDF 2022 M_W inputs, respectively.



Supplementary Figure 5. Correlation between the muon $g - 2$ and $BR(h \rightarrow \mu\mu)$. Correlation between the muon $g - 2$ and the branching ratio $BR(h \rightarrow \mu\mu)$ normalized to its SM value in our leptoquark model. The gray line shows the relationship without the contribution from left-handed couplings ($\lambda_L = 0$), while the green, red, and blue lines correspond to $\lambda_L = 10^{-2}$, 5×10^{-2} and 10^{-1} , respectively. The mass splitting is fixed at 30 GeV to be compatible with the W mass measurement. The upper limit on the branching ratio excludes the brown region, whereas the required muon $g - 2$ is shown by the purple region.